Synthesis via RAFT Polymerization of Tadpole-Shaped Organic/Inorganic Hybrid Poly(acrylic acid) Containing Polyhedral Oligomeric Silsesquioxane (POSS) and Their Self-assembly in Water

Weian Zhang,[†,‡] Bing Fang,[†] Andreas Walther,[†] and Axel H. E. Müller*[,†]

Makromolekulare Chemie II, Universität Bayreuth, D-95440 Bayreuth, Germany, and Laboratory for Advanced Materials, Department of Chemistry, East China University of Science and Technology, 130 Meilong Road, Shanghai 200237, P. R. China

Received December 16, 2008; Revised Manuscript Received February 17, 2009

ABSTRACT: Tadpole-shaped inorganic/organic hybrid poly(*tert*-butyl acrylate) was prepared by RAFT polymerization of *tert*-butyl acrylate (*t*BA) using a POSS-containing chain transfer agent (CTA). The polymerization kinetics showed a pseudofirst-order behavior with a short induction period; the number-average molecular weights linearly increase with conversion. In conjunction with low polydispersity (PDI < 1.3), this confirms a controlled polymerization. POSS-P*t*BA was further hydrolyzed into amphiphilic, tadpole-shaped poly(acrylic acid) (POSS-PAA). The self-assembly behavior of POSS-PAA in aqueous solution at pH = 8.5 was investigated by transmission electron microscopy (TEM) as well as static and dynamic light scattering (SLS and DLS). The results show that POSS-PAA self-assembles in water into rather large aggregates where the POSS moieties are dispersed in the particle. The size (average radius ≈ 60 nm by DLS) is nearly independent of the chain length of PAA. The aggregates are pH-responsive, contracting when decreasing pH from 8.5 to 4.

Introduction

Organic−inorganic hybrid materials have attracted great interest in recent years, due to the combination of properties derived from the organic and inorganic components.[1−5] Polyhedral oligomeric silsesquioxanes (POSS), a class of unique inorganic components, can be incorporated into polymer matrices to produce many novel hybrid polymers with advantageous properities.[6−9] POSS molecules have a cage-shaped three-dimensional structure with the formula $(RSiO_{1.5})_n$, ($n \geq 6$). Among them, octasilsesquioxanes ($R_8Si_8O_{12}$) ($n = 8$) have been mostly investigated; they consist of a rigid, cubic silica core with a 0.53 nm side length, where each of the eight corners carries one organic group. The corner groups can be reactive or unreactive groups, which provide the POSS molecules with the higher reactivity and solubility in organic solvents.[10−12] Thus, the POSS molecules are much more variable in their properties as compared to other inorganic components, such clays or carbon nanotubes. POSS molecules can be incorporated into almost all kinds of the polymer matrices by blending, grafting, cross-linking or copolymerization, to produce POSS-containing organic−inorganic hybrids with many promising properties such as enhanced mechanical and thermal properties, oxidation resistance, and reduced flammability.[6−9,13−28]

In previous research, much attention has been focused on the preparation methods and the properties of POSS-containing hybrid polymers. For example, atom-transfer radical polymerization (ATRP) has been used to prepare POSS-containing hybrid polymers with different topological structures such as star-shaped, block and tadpole-shaped hybrid polymers.[29−31] Telechelic and hemitelechelic POSS-containing hybrid polymers were also synthesized by urethane formation between hydroxy-terminal polymers and isocyanate group of POSS molecules.[32−35] However, there are still many other novel aspects worthy to be studied, especially the self-assembly behavior of these hybrid polymers with novel architectures. POSS molecules were also used to modify polystyrene-*block*-polybutadiene-*block*-polystyrene (SBS) triblock copolymers and the bulk morphology of the block copolymers was still preserved.[36,37] Zhu et al. investigated the self-assembly and chain-folding in well-defined oligomeric polyethylene-*block*-poly(ethylene oxide)-*block*-POSS (PE-*b*-PEO-*b*-POSS) triblock co-oligomers.[38] Pyun and Matyjaszewski first reported the synthesis of ABA triblock copolymers with a POSS-containing methacrylate monomer via ATRP, and the self-assembly structure formed in thin films.[39,40] POSS-containing diblock copolymers were also prepared by anionic polymerization and lamellar bulk structures were observed.[41] Recently, W. Zhang et al. synthesized tadpole-shaped hybrid poly(*N*-isopropylacrylamide) (PNIPAAm) using a POSS-containing reversible addition-fragmentation transfer (RAFT) agent.[42] The tadpole-shaped POSS-PNIPAAm self-assembles into core−shell nanostructured micelles with uniform diameter.

In this contribution, we extend the study of the self-assembly of POSS-containing hybrid polymers toward polyelectrolytes. We synthesized amphiphilic POSS-containing tadpole-shaped hybrid poly(acrylic acid) (PAA) using RAFT polymerization of *tert*-butyl acrylate (*t*BA). The POSS-PAA was prepared via the hydrolysis of POSS-P*t*BA using trifluoroacetic acid. The self-assembly behavior of the hybrid POSS-PAA was investigated by transmission electron microscopy (TEM) and light scattering (DLS and SLS).

Experimental Section

Materials. Aminoisobutyl polyhedral oligomeric silsesquioxane (POSS) was purchased from Hybrid Plastics Company. *tert*-Butyl acrylate (*t*BA) was kindly supplied by BASF SE, and was passed through an silica column to remove the inhibitor. Other regents in analytical grade were all obtained from Aldrich. Azobisisobutyronitrile (AIBN) was recrystallized from ethanol. Dichloromethane was dried over CaH_2 and distilled before use. The RAFT agent, 3-benzylsulfanylthiocarbonylsufanylpropionic acid (BSPA), was synthesized according to the literature.[43]

3-Benzylsulfanylthiocarbonylsufanyl-N-(3-(isobutyl polyhedral oligomeric silsesquioxane) propyl)propanamide (POSS-BSPA). The synthesis of the POSS-containing RAFT agent, POSS-BSPA, was

* Corresponding author. E-mail: axel.mueller@uni-bayreuth.de.
† Makromolekulare Chemie II, Universität Bayreuth.
‡ Laboratory for Advanced Materials, Department of Chemistry, East China University of Science and Technology.

10.1021/ma802803d CCC: $40.75
Published on Web 03/10/2009

reported in our previous paper.[42] The resulting product was further crystallized in petroleum ether with a yield of 80%. ^{1}H NMR ($CDCl_3$, ppm): 7.27−7.34 (m, 5*H*, Ph), 4.61 (s, 2*H*, CH_2Ph), 3.67 (t, 2*H*, −Si−$CH_2CH_2CH_2$NH−), 3.25 (q, 2*H*, −HNCOCH_2CH_2S−), 2.60 (t, 2*H*, −HNCOCH_2CH_2S−), 1.85 (m, 7*H*, −Si−$CH_2CH(CH_3)_2$), 1.60 (m, 2*H*, −Si−$CH_2CH_2CH_2$NH−), 0.95 (d, *42H*, −Si−$CH_2CH(CH_3)_2$), 0.60 (m, *16H*, −Si−$CH_2CH(CH_3)_2$, −Si−$CH_2CH_2CH_2$NH−).

Synthesis of POSS-P*t*BA. A typical polymerization procedure for the synthesis of POSS-containing inorganic/organic hybrid P*t*BA as follows: A round-bottom glass flask (50 mL) with a magnetic stir bar was charged with *t*BA (3 mL, 20.67 mmol), POSS-containing RAFT agent (125.5 mg, 0.11 mmol), AIBN (6.08 mg, 0.037 mmol) and 15 mL of toluene. The mixture solution was purged with argon for 30 min, and then the glass tube was sealed under argon. The polymerization was carried out in a thermostatted oil bath at 70 °C. Small samples (about 0.5 mL) were taken out from the reaction flask at intervals to check the conversion, which was measured by ^{1}H NMR by comparing the peaks of the double bond protons of *t*BA at 5.75 ppm and of the toluene aromatic protons at 7.23 ppm. At the end of the polymerization reaction, the polymerization was stopped by plunging the tube into ice water. The polymerization flask was opened, and then precipitated into 250 mL cold mixed solution of methanol/water (3/1, v/v). The precipitate was redissolved in dioxane, and the product was dried by freeze-drying for two days. ^{1}H NMR (dioxane-d_8, ppm): 7.15−7.23 (m, 5*H*, Ph), 2.10−2.35, 1.65−1.93 (m, polymer backbone protons, −Si−$CH_2CH(CH_3)_2$), 1.44 (s, −$COO(CH_3)_3$), 0.97 (d, −Si−$CH_2CH(CH_3)_2$)), 0.62 (m, −Si−$CH_2CH(CH_3)_2$, −Si−$CH_2CH_2CH_2$NH−). M_n(GPC) = 15 870, M_w/M_n = 1.20.

Preparation of POSS-PAA from POSS-P*t*BA. A typical procedure for the conversion of POSS-P*t*BA to POSS-PAA as follows: a round-bottom flask (50 mL) with a magnetic stir bar was charged with POSS-P*t*BA_{60} (M_n = 8, 374, 0.5 g, 3.4 mmol of *tert*-butyl acrylate unit) followed by dichloromethane (40 mL). The mixture was allowed to stir for 15 min to dissolve the polymer. And then trifluoroacetic acid (TFA; 4.0 mL, 53.0 mmol) was added. The mixture was allowed to stir at room temperature for 24 h. After 24 h, a yellow precipitate had formed, and dichloromethane and TFA were removed by rotary evaporation. The product was washed three times with dichloromethane, and then redissolved in dioxide, and followed by freeze-drying to afford the light yellow powder. ^{1}H NMR (dioxane-d_8, ppm): 7.15−7.23 (m, 5*H*, Ph), 2.20−2.53, 1.37−1.93 (m, polymer backbone protons, −Si−$CH_2CH(CH_3)_2$), 0.97 (d, −Si−$CH_2CH(CH_3)_2$)), 0.62 (m, −Si−$CH_2CH(CH_3)_2$, −Si−$CH_2CH_2CH_2$NH-)). M_n=4,953, M_w/M_n=1.10 (MALDI−TOF).

Self-assembly of POSS-PAA in Aqueous Solution. A typical self-assembly aggregate solution was prepared as following: POSS-PAA_{60} (100 mg) was first dissolved in dioxane (25 mL), which is a good solvent for POSS-PAA. The solution was stirred overnight, and gradually dialyzed against pH 8.5 Millipore water (resistance = 18 MΩ) for 3 days. After gradual dialysis, the self-assembly aggregate solution was dialyzed at least three times using pH 8.5 Millipore water to make sure to completely remove dioxane.

Characterization

Nuclear Magnetic Resonance Spectroscopy (NMR). The ^{1}H NMR and ^{13}C NMR measurements were carried out on a Bruker AC-250 instrument. The samples were dissolved in deuterated $CDCl_3$ and dioxane-d_8, respectively, and the solutions were measured with tetramethylsilane (TMS) as an internal reference. By comparing the peaks of the polymer backbone methine protons at 2.22 ppm and the *tert*-butyl protons at 1.45 ppm with the methyl protons of the hepta(isobutyl) groups of POSS at 0.97 pm, the number-average degrees of polymerization and the corresponding molecular weights were determined as $M_{n,NMR} = [((I_{1.45}/9) + I_{2.22})/2]/[I_{0.97}/42] \times M_{tBA} + M_{CTA.}$, where, M_{tBA} and M_{CTA} are the molecular weights of monomer and CTA, respectively. ^{29}Si NMR spectra were measured on a Varian Inova 300 MHz spectrometer at 23 °C. The samples were dissolved in dioxane-d_8; chemical shifts are given relative to TMS [δ^{29}Si = 0 ppm for $\Xi(^{29}Si)$ = 19.867184 MHz]; Chemical shifts are given to ± 0.1 for ^{29}Si; coupling constants are given ± 0.4 Hz for $J(^{29}Si)$. The spectra were measured by using the refocused INEPT pulse sequence based on $^{2/3}J(^{29}Si)$ = 10 Hz after optimizing the delay times in the pulse sequence.

Fourier Transform Infrared Spectroscopy (FTIR). Measurements were conducted on a Bruker Equinox 55/s Fourier transform spectrometer at room temperature (25 °C). The samples mixed with KBr were granulated into powder and pressed into flakes for IR measurements.

Gel Permeation Chromatography (GPC). The molecular weights and molecular weight distribution were measured by conventional GPC. Column set: 5 μm SDV gel, 10^2, 10^3, 10^4, and 10^5 Å, 30 cm each (PSS, Mainz). Detectors used are RI and UV operated at 254 nm. Polystyrene standards (PSS, Mainz) with narrow molecular weight distribution were used for the calibration of the column set, and tetrahydrofuran (THF) was used as the eluent at a flow rate of 1 mL/min. Since the calibration curve of P*t*BA is different from that of PS, we used the number-average molecular weights obtained from the NMR signals of POSS and P*t*BA.

MALDI−TOF Mass Spectrometry. MALDI−TOF mass spectrometry was performed on a Bruker Reflex III instrument equipped with a 337 nm N_2 laser in the reflector mode and 20 kV acceleration voltage. 2,5-Dihydroxybenzoic acid (Aldrich, 97%) was used as a matrix. Samples were prepared from THF solution by mixing matrix (20 mg/mL) and polymer (10 mg/mL) in a ratio of 4:1. The number-average molecular weights of the polymers were determined in the linear mode.

Transmission Electron Microscopy (TEM) images were taken out on a Philips CM 20 TEM operated at 200 kV. A 5 μL droplet of self-assembly aggregate solution (0.5 mg/mL) was directly dropped onto a copper grid (300 mesh) coated with a carbon film, followed by drying at room temperature.

Cryogenic Transmission Electron Microscopy (cryo-TEM). The sample was prepared as described above. To achieve the desired ionic strength, CsCl (Acros) was used. A drop of the sample (concentration around 4.0 mg/mL) was directly put on a lacey grid, where most of the liquid was removed with blotting paper, leaving a thin film stretched over the lace. The specimens were instantly shock vitrified by rapid immersion into liquid ethane and cooled to approximately 90 K by liquid nitrogen in a temperature-controlled freezing unit (Zeiss Cryobox, Zeiss NTS GmbH, Oberkochen, Germany). The temperature was monitored and kept constant in the chamber during all the sample preparation steps. After the sample is frozen, it was inserted into a cryo-transfer holder (CT3500, Gatan, München, Germany) and transferred to a Zeiss EM922 EFTEM. Examinations were carried out at temperatures around 90 K at an acceleration voltage of 200 kV. Zero-loss filtered images (ΔE = 0 eV) were taken under reduced dose conditions (100−1000 electrons/nm^2). All images were registered digitally by a bottom-mounted CCD camera system (Ultrascan 1000, Gatan) combined and processed with a digital imaging processing system (Gatan Digital Micrograph 3.10 for GMS 1.5).

Dynamic Light Scattering (DLS) was carried out on an ALV DLS/SLS-SP 5022F compact goniometer system with an ALV 5000/E correlator and a He−Ne laser (λ = 632.8 nm). Before the light scattering measurements, the sample solutions were filtered three times by using Millipore Teflon (Nylon) filters with a pore size of 0.45 μm. A CONTIN analysis was taken for the measured intensity correlation functions. Apparent hydrodynamic radii, R_h, of the self-assembly aggregates were calculated according to the Stokes−Einstein equation. All measurements were carried out at room temperature. The

Scheme 1. Synthesis of POSS-Containing Poly(acrylic acid) Using a POSS-Containing RAFT Agent

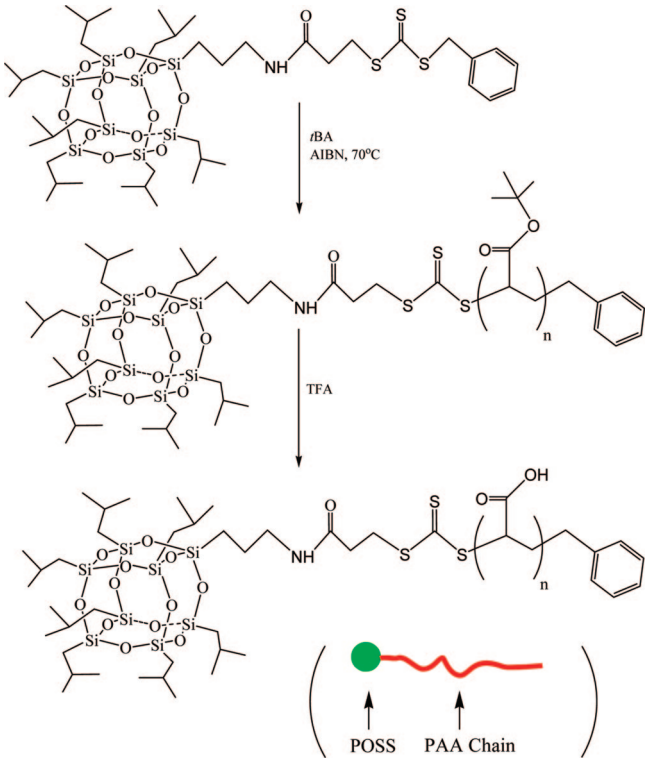

measurements were performed at fixed scattering angle of 90°. The polymer solutions had a concentration of 2 mg/mL.

Static Light Scattering (SLS) was measured on a Sofica goniometer using a He−Ne laser ($\lambda = 632.8$ nm). Prior to the light scattering measurements, the sample solutions were filtered three times by using Millipore Teflon (Nylon) filters with a pore size of 0.45 μm. Five concentrations of the polymer in aqueous solution were measured at angles in the range from 30 to 150°. Weight-average molecular weights, M_w, of the self-assembly aggregates were obtained by the analysis of the Zimm plots. The refractive index increment of the POSS-PAA aggregates in aqueous solution at 25 °C was measured using a PSS DnDc-2010/620 differential refractometer, and the d*n*/d*c* of POSS-PAA_{35} and POSS-PAA_{60} are 0.1065 and 0.1119 mL/g, respectively.

Results and Discussion

RAFT Polymerization of *t*BA Using a POSS-Containing RAFT Agent. The detailed description of the synthesis of the POSS-containing RAFT was reported in our previous paper.[42]

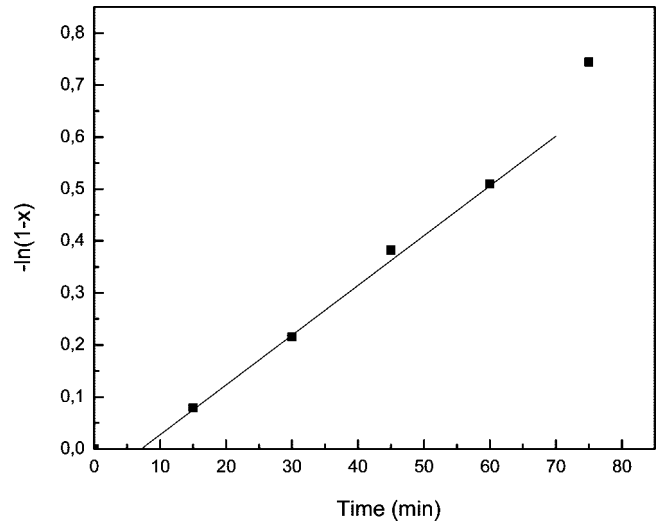

Figure 1. Pseudofirst-order kinetic plot of the preparation of POSS-P*t*BA at 70 °C in toluene in the presence of POSS-containing RAFT agent.

The NMR and IR results confirmed the POSS-containing RAFT agent was successfully prepared. To obtain POSS-containing PAA (POSS-PAA), POSS-containing P*t*BA was synthesized in advance using POSS-containing RAFT agent via RAFT polymerization. The POSS-containing P*t*BA was further hydrolyzed into POSS-containing PAA by trifluoroacetic acid in dichloromethane (Scheme 1). All polymerizations of *t*BA were carried out in toluene using AIBN as initiator. The polymerization conversion at intervals was measured by ^{1}H NMR. The polymerization results were listed in Table 1.

The kinetic plot of the polymerization of *t*BA is shown in Figure 1. A linear relationship exists between $\ln(1/(1-x))$ and reaction time, indicating that the concentration of chain radicals is constant. Thus the polymerization follows pseudofirst-order kinetics. A short induction period is observed, typical of many RAFT polymerizations and can be explained by the slow fragmentation of the intermediate radical at the early stage of RAFT polymerization.[42]

Figure 2 shows the evolution of GPC chromatograms with reaction time. With the increasing reaction times, the chromatograms shift to lower elution volume. The **r**elationships of number-average molecular weight and polydispersity index (PDI) versus monomer conversion are shown in Figure 3. The molecular weight linearly increases with conversion but differs from the theoretical values (see also Table 1). This might indicate a so-called hybrid behavior as proposed by Barner-Kowollik et al., meaning that in the initial stage of polymerization the system acts similar to a conventional polymerization

Table 1. Conditions and Results of the RAFT Polymerization of *t*BA Using a POSS-Containing RAFT Agent[a]

samples	$[M]_0/[CTA]_0$[a]	T (°C)	time (min)	conversion (%)	$10^{-3}\ M_{n,th}$[b]	$10^{-3}M_n$ (NMR)[c]	$10^{-3}M_n$ (GPC)[d]	M_w/M_n[d]
1[e]	186	70	15	7.6	2.94	5.79	4.71	1.20
2[e]	186	70	30	19.4	5.75	6.61	5.71	1.21
3[e]	186	70	45	31.8	8.70	8.09	7.53	1.18
4[e]	186	70	60	40.0	10.7	9.47	9.22	1.17
5[e]	186	70	75	52.5	13.6	10.63	10.64	1.15
POSS-P*t*BA_{107}[f]	186	70	275	78.5	19.8	14.89	15.87	1.20
POSS-P*t*BA_{136}[f]	186	80	210	92.0	23.1	18.56	20.37	1.19
POSS-P*t*BA_{60}[f]	93	70	275	85.7	11.3	8.78	8.37	1.23
POSS-P*t*BA_{35}[f]	46	70	275	94.4	6.75	5.62	4.49	1.30
BSPA-P*t*BA[g]	93	70	275	90.9	11.1		6.52	1.39

[a] In toluene, $[M]_0 = 1.38$ mol/L; $[CTA]/[AIBN] = 3$. [b] Calculated as $M_{n,th} = [M]_0/[CTA]_0 \times M_{tBA} \times x + M_{CTA}$, where [M] and [CTA] are respectively the initial concentrations of the *t*BA and RAFT agent, M_{tBA} is the molecular weight of *t*BA, and M_{CTA} is the molecular weight of RAFT agent and x is the conversion. [c] determined from the ^{1}H NMR spectra. [d] Measured by GPC calibrated with PS standards. [e] Kinetic runs. [f] The numbers behind POSS-P*t*BA correspond to the degree of polymerization, as determined from ^{1}H NMR. [g] BSPA is 3-benzylsulfanylthiocarbonylsulfanylpropionic acid (reference CTA without POSS).

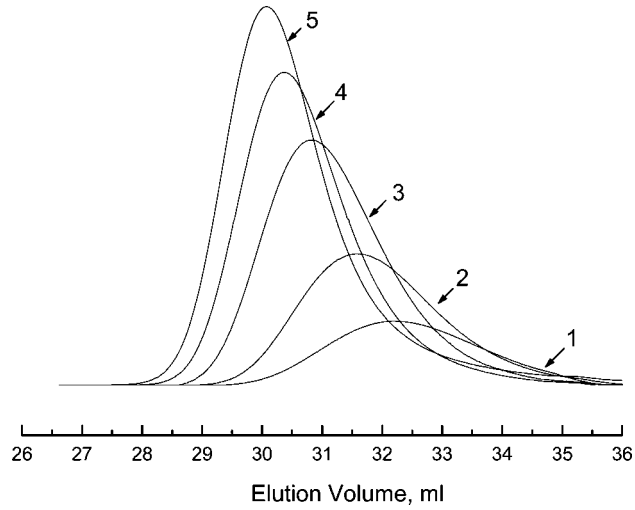

Figure 2. Evolution of GPC chromatograms for the RAFT polymerization of *t*BA at 70 °C in toluene after different reaction times in the presence of POSS-containing RAFT agent (Table 1, entries 1−5).

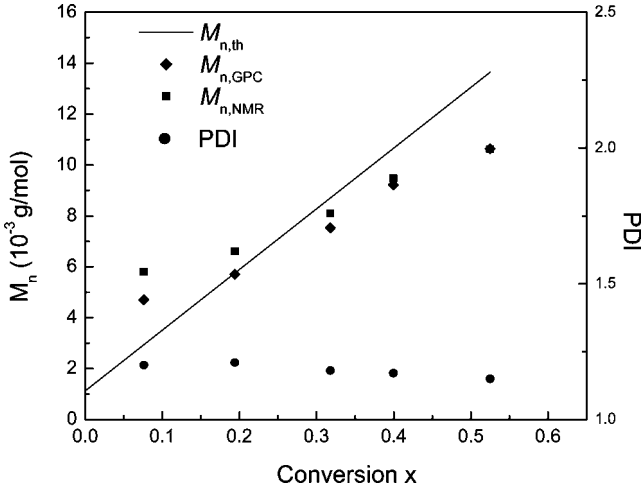

Figure 3. Evolution of number-average molecular weight and polydispersity with conversion for the RAFT polymerization of *t*BA at 70 °C in toluene in the presence of POSS-containing RAFT agent.

and then converts to a controlled one.[44,45] It could also be related to a change in the structure of the POSS-functional P*t*BA, which might result in a different hydrodynamic volume compared to P*t*BA homopolymer. A similar observation was made by Mather et al.[32,33]

The GPC traces of the control P*t*BA and all POSS-containing hybrid P*t*BAs prepared with different amount of RAFT agents are symmetrical, with no shoulder and tail appearing. All the results stated above indicate that the controlled nature of the RAFT polymerization of *t*BA and that the POSS-containing CTA is effective in the RAFT polymerization of *t*BA.

The characteristic signals in the ^{1}H NMR spectrum of P*t*BA$_{60}$ (Figure S1 in the Supporting Information) at $\delta = 2.23$ ppm (d) and 1.45 ppm (f), are ascribed to the methine protons of the backbone and the methyl protons of the *tert*-butyl groups, respectively. The protons signals of the POSS-CTA can be identified at $\delta = 0.97$ ppm (a) and 0.62 ppm (c), which are respectively assigned to the methyl ($-$Si$-$CH_2CH(CH_3)$_2$) and methylene ($-$Si$-$CH_2CH(CH$_3$)$_2$, $-$Si$-$CH_2CH_2CH$_2$NH$-$) protons. This further confirms that POSS-P*t*BA was successfully synthesized.

Preparation of POSS-PAA from POSS-P*t*BA Using TFA. POSS-PAA was obtained by hydrolysis of the *tert*-butyl ester groups of POSS-P*t*BA in dichloromethane using trifluoroacatic acid (TFA), which is a well-known method to afford amphiphilic block copolymers containing a PAA block.[46−48] At first, we worried that the trithioester and the POSS moiety might become destroyed by TFA. However, during the hydrolysis, a light yellow precipitation gradually appeared, and the solution remained colorless, which suggests that the trithiocarbonate was unaffected by TFA. Moreover, IR and NMR results show that POSS-P*t*BA was completely transformed into POSS-PAA, and the POSS molecule was not degraded in the hydrolysis, indicating that it is an effective method to afford POSS-PAA. The deformation vibration of the *tert*-butyl group at 1369 cm^{-1} completely disappeared in the IR spectrum of POSS-PAA (Figure S2). Moreover, the carbonyl absorbance peak at 1729 cm^{-1} slightly shifts to lower wavenumbers, and the peak also becomes broader, attributed to the formation of carboxylic acid from the *tert*-butyl ester. In addition, we also can see a broad absorbance peak at the in the range from 2317 to 3707 cm^{-1} in the spectrum of POSS-PAA, which is mainly due to the formation of carboxylic acid groups.

The ^{1}H NMR spectrum of POSS-PAA also shows that the proton signal of the *tert*-butyl ester groups at 1.45 ppm completely disappeared after the hydrolysis (Figure S3). The ^{13}C NMR spectrum also shows the carbon resonance for the *tert*-butyl ester at 28.2 and 80.12 ppm in spectrum of POSS-P*t*BA (Figure S4) completely disappeared in the spectrum of POSS-PAA (Figure S5). Thus, on the basis of the IR and NMR results, POSS-P*t*BA was completely hydrolyzed into POSS-PAA. Comparing the ^{1}H NMR spectrum of POSS-P*t*BA with that of POSS-PAA, the characteristic proton signals of the POSS molecule at $\delta = 0.97$ ppm (a) and 0.62 ppm (c) are almost unchanged in the two spectra. We also observe there is no change for the characteristic silicon resonace of POSS at $\delta = -63.8$ ppm and -64.1 ppm in the two ^{29}Si NMR spectra (Figure S6). This suggests that there is no degradation of the POSS molecule in the hydrolysis of *tert*-butyl groups. In addition, MALDI−TOF mass spectrometry was used to characterize the molecular weight of POSS-PAA, and the molecular weight is close to the theoretically calculated one, which further confirms that POSS-PAA was successfully prepared (Figure S7).

Scheme 2. Self-Assembly Process of POSS-Containing Hybrid Poly(acrylic acid) in Aqueous Solution

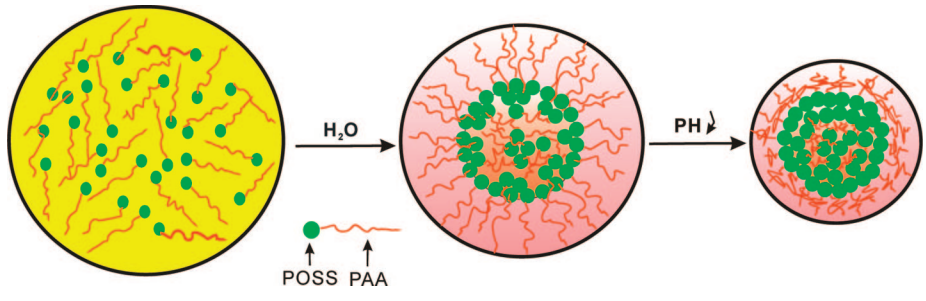

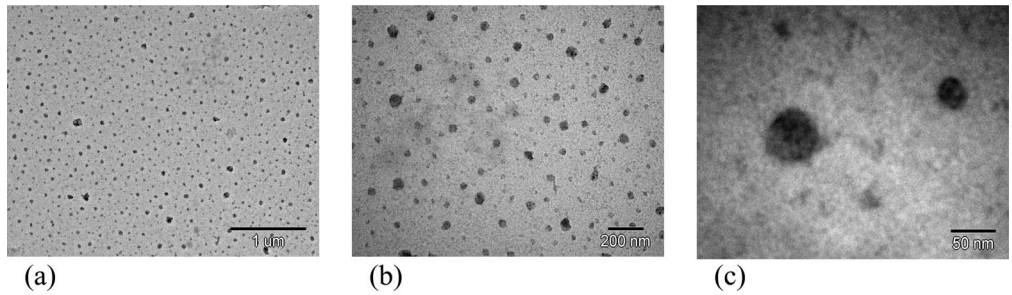

Figure 4. TEM images of POSS-PAA_{60} self-assembly aggregates at different magnifications with pH = 8.5.

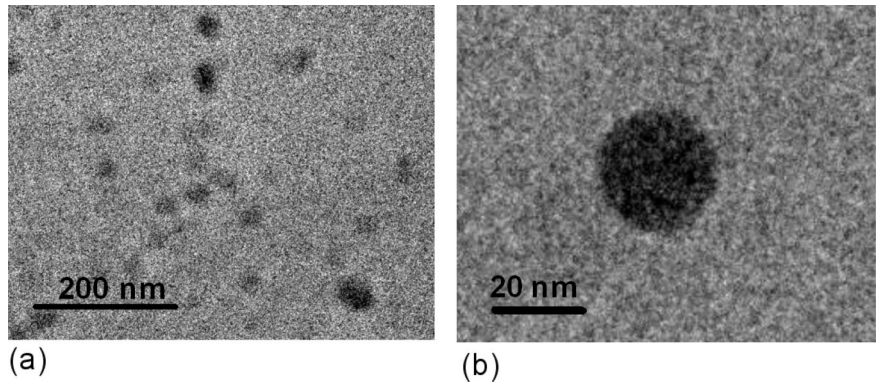

Figure 5. Cryo-TEM of POSS-PAA_{136} self-assembly aggregates at different magnifications with pH = 8.5.

Self-Assembly Behavior of POSS-Containing Hybrid Poly(acrylic acid). The self-assembly of amphiphilic polymers has attracted considerable attention in polymer science, since it can result in the formation of a rich variety of microdomain morphologies such as spheres, cylinders, lamellae and gyroids in bulk or solution.[49−52] Whereas the polymers used in self-assembly are mostly prepared from organic molecules, inorganic hydrophobes have been rarely reported. Amphiphilic polymers based on poly(acrylic acid) (PAA) are well-known representatives in the study of the self-assembly of ionic amphiphilic block polymers.[53,54] In this work, the tadpole-shaped inorganic/organic hybrid POSS-PAA is similar to an amphiphilic block copolymer, since the POSS molecule is hydrophobic and the PAA chain is hydrophilic (Scheme 2).

Transmission electron micrioscopy (TEM) was used to characterize the morphology of the POSS-PAA self-assembly aggregates. The sample was prepared by directly dropping the polymer solution on the carbon-coated copper grid without additional staining or etching. Parts a−c of Figure 4 show the TEM images of POSS-PAA_{60} self-assembly aggregates at different magnifications. Figure 4a shows that the aggregates are well-dispersed, however they are quite polydisperse in size (radii from 15 to 42 nm). From the enlarged image (Figure 4c) we observe that the density of the aggregate is not uniform, which may indicate that POSS-PAA in aqueous solution does not self-assemble into the typical core−shell micelles with POSS molecules as the core and PAA as the shell, but rather aggregates (Scheme 2). This structure is further confirmed by cryogenic TEM (Figure 5). There is no typical core−shell structure in the image. The density of the aggregates is also not uniform in a single aggregate (Figure 5b).

The self-assembly aggregate solutions were also measured by DLS (Figure 6). The apparent hydrodynamic radii, R_h, are considerably larger than those measured by TEM. This can be attributed to the fact that the hydrodynamic radii are z-averages and the PAA chains are extended in solution. The values of

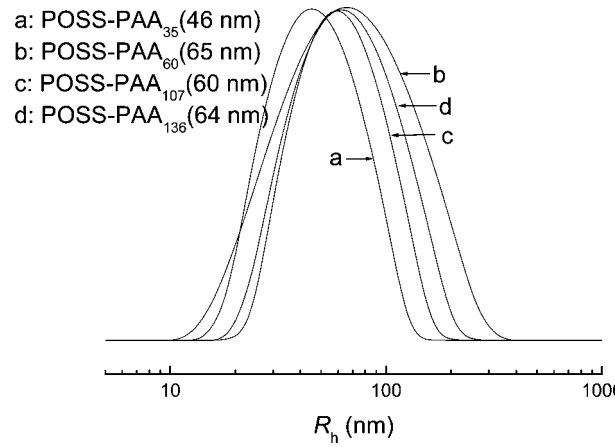

Figure 6. Intensity-weighted hydrodynamic radius distributions of POSS-PAA self-assembly aggregates and z-average hydrodynamic radii in aqueous solution at pH = 8.5 and 90° measurement angle.

46−64 nm are much larger than those of one extended PAA chain (0.25 nm x DP, i.e. between 9 and 34 nm). The cumulant analysis renders rather large polydisperity values in the range from 0.3 to 0.5. In addition, the radii do not significantly depend on the chain length of PAA, except for the lowest one (Figure 6). This further suggests different aggregation numbers, N_{agg}, for different PAA molecular weights. SLS measurements give the apparent molecular weights, $M_{w,app}$, of aggregates of POSS-PAA_{35} and POSS-PAA_{60} as 2.69×10^6 g/mol and 4.85×10^6 g/mol, respectively. The average N_{agg} of the aggregates of POSS-PAA_{35} and POSS-PAA_{60} are estimated as 480 and 550, respectively. This large aggregation number cannot be explained by a simple core−shell aggregate structure since the core of such an aggregate must contain a considerable amount of PAA, which is attached to the POSS moieties. Thus, we have to assume that the particles are rather aggregates with a distribution

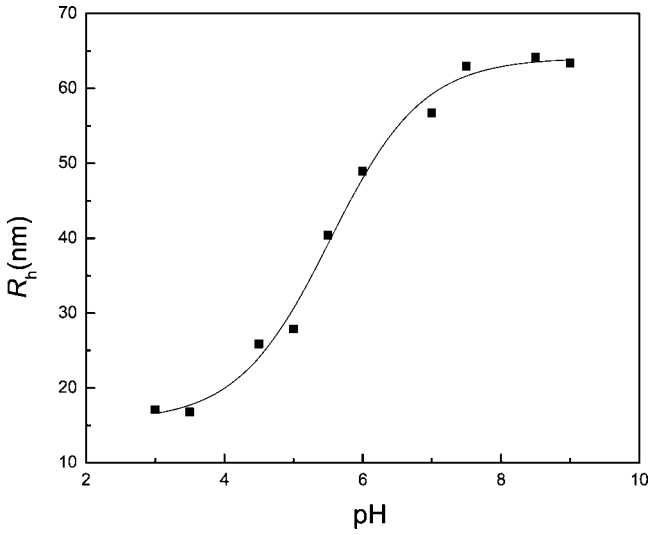

Figure 7. Dependence of hydrodynamic radius of POSS-PAA$_{136}$ self-assembly aggregates on pH.

of POSS moieties within the aggregate, as is also indicated by the TEM image in Figure 4c.

The pH dependence of R_h for the POSS-PAA self-assembly aggregates is shown in Figure 7. The *z*-average hydrodynamic radius decreases when decreasing pH from 8.5 to 4, due to protonation and the resulting contraction of the PAA chains (Scheme 2). This proves that the POSS-PAA aggregates are responsive to pH, similar to organic core−shell micelles of polystyrene-*block*-PAA (PS-*b*-PAA) or polyisobutylene-*block*-poly(methacrylic acid) (PIB-*b*-PMAA) diblock copolymers.[55,56]

Conclusions

POSS-containing tadpole-shaped organic/inorganic hybrid P*t*BA was successfully obtained using a POSS-containing RAFT agent. The polymerization is well-controlled. POSS-P*t*BA was completely transformed to POSS-PAA. TEM and light scattering results show that POSS-PAA self-assembles in water into a structure that is different from a simple core−shell micelle with POSS molecules as the core and PAA as the shell. Apparently aggregates are formed where the POSS moieties are dispersed in the particle. The size of these aggregates, being pH-responsive, does not significantly depend on the DP of the PAA chains.

Acknowledgment. This work was supported by the Alexander von Humboldt Foundation. W.Z. also acknowledges support by the National Natural Science Foundation of China (No. 50503013). We thank Ms. Anja Goldmann for the MALDI−TOF MS measurements and Mr. Ezzat Khan (Inorganic Chemistry) for performing the ^{29}Si NMR measurements. W.Z. acknowledges Mr. Youyong Xu and Mr. Jiayin Yuan for help and discussions.

Supporting Information Available: Figures showing FTIR, ^{1}H, ^{13}C NMR and ^{29}Si NMR spectra of POSS-P*t*BA and POSS-PAA and MALDI−TOF mass spectrum of POSS-PAA. This material is available free of charge via the Internet at http://pubs.acs.org.

References and Notes

(1) Giannelis, E. P.; Krishnamoorti, R.; Manias, E. *Adv. Polym. Sci.* **1999**, *138*, 107–147.
(2) Kickelbick, G. *Prog. Polym. Sci.* **2003**, *28*, 83–114.
(3) Abe, Y.; Gunji, T. *Prog. Polym. Sci.* **2004**, *29*, 149–182.
(4) Baney, R. H.; Itoh, M.; Sakakibara, A.; Suzuki, T. *Chem. Rev.* **1995**, *95*, 1409–1430.
(5) Sun, Y. P.; Fu, K. F.; Lin, Y.; Huang, W. J. *Acc. Chem. Res.* **2002**, *35*, 1096–1104.
(6) Pielichowski, K.; Njuguna, J.; Janowski, B.; Pielichowski, J. *Adv. Polym. Sci.* **2006**, *201*, 225–296.
(7) Li, G. Z.; Wang, L. C.; Ni, H. L.; Pittman, C. U. *J. Inorg. Organomet. Polym.* **2001**, *11*, 123–154.
(8) Phillips, S. H.; Haddad, T. S.; Tomczak, S. J. *Curr. Opin. Solid State Mater. Sci.* **2004**, *8*, 21–29.
(9) Laine, R. M. *J. Mater. Chem.* **2005**, *15*, 3725–3744.
(10) Sprung, M. M.; Guenther, F. O. *J. Am. Chem. Soc.* **1955**, *77*, 3990–3996.
(11) Brown, J. F. *J. Am. Chem. Soc.* **1965**, *87*, 4317–4324.
(12) Lichtenhan, J. D.; Schwab, J. J.; Feher, F. J.; Soulivong, D. *US Patent 5,942,638*, **1999**.
(13) Constable, G. S.; Lesser, A. J.; Coughlin, E. B. *Macromolecules* **2004**, *37*, 1276–1282.
(14) Lee, A.; Xiao, J.; Feher, F. J. *Macromolecules* **2005**, *38*, 438–444.
(15) Cho, H. J.; Hwang, D. H.; Lee, J. I.; Jung, Y. K.; Park, J. H.; Lee, J.; Lee, S. K.; Shim, H. K. *Chem. Mater.* **2006**, *18*, 3780–3787.
(16) Kang, J. M.; Cho, H. J.; Lee, J.; Lee, J. I.; Lee, S. K.; Cho, N. S.; Hwang, D. H.; Shim, H. K. *Macromolecules* **2006**, *39*, 4999–5008.
(17) Chou, C. H.; Hsu, S. L.; Dinakaran, K.; Chiu, M. Y.; Wei, K. H. *Macromolecules* **2005**, *38*, 745–751.
(18) Kopesky, E. T.; Haddad, T. S.; Cohen, R. E.; McKinley, G. H. *Macromolecules* **2004**, *37*, 8992–9004.
(19) Abad, M. J.; Barral, L.; Fasce, D. P.; Williams, R. J. J. *Macromolecules* **2003**, *36*, 3128–3135.
(20) Mabry, J. M.; Vij, A.; Iacono, S. T.; Viers, B. D. *Angew. Chem., Int. Ed.* **2008**, *47*, 4137–4140.
(21) Xu, H. Y.; Kuo, S. W.; Lee, J. S. Y.; Chang, F. C. *Macromolecules* **2002**, *35*, 8788–8793.
(22) Kotal, A.; Si, S.; Paira, T. K.; Mandal, T. K. *J. Polym. Sci., Part A: Polym. Chem.* **2008**, *46*, 1111–1123.
(23) Strachota, A.; Whelan, P.; Kriz, J.; Brus, J.; Urbanova, M.; Slouf, M.; Matejka, L. *Polymer* **2007**, *48*, 3041–3058.
(24) Liu, H. Z.; Zheng, S. X.; Nie, K. M. *Macromolecules* **2005**, *38*, 5088–5097.
(25) Knight, P. T.; Lee, K. M.; Qin, H.; Mather, P. T. *Biomacromolecules* **2008**, *9*, 2458–2467.
(26) Markovic, E.; Matisons, J.; Hussain, M.; Simon, G. P. *Macromolecules* **2007**, *40*, 4530–4534.
(27) Paul, R. K. U.; Swift, M. C.; Esker, A. R *Langmuir* **2008**, *24*, 5079–5090.
(28) Hottle, J. R.; Deng, J.; Kim, H. J.; Farmer-Creely, C. E.; Viers, B. D.; Esker, A. R. *Langmuir* **2005**, *21*, 2250–2259.
(29) Costa, R. O. R.; Vasconcelos, W. L.; Tamaki, R.; Laine, R. M. *Macromolecules* **2001**, *34*, 5398–5407.
(30) Pyun, J.; Matyjaszewski, K. *Macromolecules* **2000**, *33*, 217–220.
(31) Ohno, K.; Sugiyama, S.; Koh, K.; Tsujii, Y.; Fukuda, T.; Yamahiro, M.; Oikawa, H.; Yamamoto, Y.; Ootake, N.; Watanabe, K. *Macromolecules* **2004**, *37*, 8517–8522.
(32) Kim, B. S.; Mather, P. T. *Macromolecules* **2002**, *35*, 8378–8384.
(33) Kim, B. S.; Mather, P. T. *Polymer* **2006**, *47*, 6202–6207.
(34) Kim, B. S.; Mather, P. T. *Macromolecules* **2006**, *39*, 9253–9260.
(35) Cardoern, G.; Coughlin, E. B. *Macromolecules* **2004**, *37*, 5123–5126.
(36) Drazkowski, D. B.; Lee, A.; Haddad, T. S.; Cookson, D. J. *Macromolecules* **2006**, *39*, 1854–1863.
(37) Drazkowski, D. B.; Lee, A.; Haddad, T. S. *Macromolecules* **2007**, *40*, 2798–2805.
(38) Miao, J.; Cui, L.; Lau, H. P.; Mather, P. T.; Zhu, L. *Macromolecules* **2007**, *40*, 5460–5470.
(39) Pyun, J.; Matyjaszewski, K. *Chem. Mater.* **2001**, *13*, 3436–3448.
(40) Pyun, J.; Matyjaszewski, K.; Wu, J.; Kim, G. M.; Chun, S. B.; Mather, P. T. *Polymer* **2003**, *44*, 2739–2750.
(41) Hirai, T.; Leolukman, M.; Hayakawa, T.; Kakimoto, M. A.; Gopalan, P. *Macromolecules* **2008**, *41*, 4558–4560.
(42) Zhang, W. A.; Liu, L.; Zhuang, X. D.; Li, X. H.; Bai, J. R.; Chen, Y. *J. Polym. Sci., Part A: Polym. Chem.* **2008**, *46*, 7049–7061.
(43) Stenzel, M. H.; Davis, T. P. *J. Polym. Sci., Part A: Polym. Chem.* **2002**, *40*, 4498–4512.
(44) Barner-Kowollik, C.; Quinn, J. F.; Morsley, D. R.; Davis, T. P. *J. Polym. Sci., Part A: Polym. Chem.* **2001**, *39*, 1353–1365.
(45) Barner-Kowollik, C., *Handbook of RAFT Polymerization*. Viley VCH: Weinheim, Germany, 2008.
(46) Eghbali, E.; Colombani, O.; Drechsler, M.; Müller, A. H. E.; Hoffmann, H. *Langmuir* **2006**, *22*, 4766–4776.
(47) Connal, L. A.; Li, Q.; Quinn, J. F.; Tjipto, E.; Caruso, F.; Qiao, G. G. *Macromolecules* **2008**, *41*, 2620–2626.
(48) Colombani, O.; Ruppel, M.; Schubert, F.; Zettl, H.; Pergushov, D. V.; Müller, A. H. E. *Macromolecules* **2007**, *40*, 4338–4350.

(49) Hamley, I. W. *The Physics of Block Copolymers*, Oxford University Press: Oxford, U.K., 1998.
(50) Alexandridis, P.; Lindman, B. *Amphiphilic Block Copolymers: Self-assembly and Applications*; Elsevier: Amsterdam, 2000.
(51) Abetz, V.; Simon, P. F. W. *Adv. Polym. Sci.* **2005**, *189*, 125–2125.
(52) Gohy, J. F. *Adv. Polym. Sci.* **2005**, *190*, 65–136.
(53) Zhang, L.; Eisenberg, A. *Science* **1995**, *268*, 1728–1731.
(54) Zhang, L.; Eisenberg, A. *J. Am. Chem. Soc.* **1996**, *118*, 3168–3181.
(55) Zhang, L. F.; Eisenberg, A. *Macromolecules* **1996**, *29*, 8805–8815.
(56) Burkhardt, M.; Martinez-Castro, N.; Tea, S.; Drechsler, M.; Babin, I. A.; Grishagin, I. V.; Schweins, R.; Pergushov, D. V.; Gradzielski, M.; Zezin, A. B.; Müller, A. H. E. *Langmuir* **2007**, *23*, 12864–12874.

MA802803D